Synthesis, spectroscopic depiction and phenoxazinone synthase activity by a cobalt(II) complex

Ajit Das[a], Anita Sahu[b], Prafullya Kumar Mudi[b], Suvendu Paul[c], Nagendranath Mahata[a] and Bhaskar Biswas[b]*

[a]Department of Chemistry, Sidho-Kanho-Birsha University, Purulia-723 104, West Bengal, India

[b]Department of Chemistry, University of North Bengal, Darjeeling-734 013, West Bengal, India

E-mail: mr.bbiswas@rediffmail.com, icbbiswas@gmail.com

[c]Department of Chemistry, University of Kalyani, Kalyani-741 235, West Bengal, India

Synthesis and structural characterization of a cobalt(II) complex, $[Co(2,2'-dpa)_2(NO_3)]NO_3$ (**1**) [2,2'-dpa = 2,2'-dipyridylamine] has been reported. Single crystal X-ray diffraction study reveals that **1** crystallizes in monoclinic system with $P2_1/n$ space group. Investigation on supramolecular investigation reveals that counter anionic nitrate ion plays a crucial role in the construction of long range 3D crystalline structure. Room temperature magnetic susceptibility measurement predicts the high spin nature of the cobalt(II) compound. The cobalt(II) complex has been evaluated to mimics the functional sites of phenoxazinone synthase enzyme in acetonitrile medium. The cobalt(II) complex significantly able to promote the oxidative coupling of 2-aminophenol (2-AP) to 2-aminophenoxazin-3-one under aerobic condition with significant turn over number, $k_{cat} = 1.46 \times 10^4$ h^{-1}. ESI-MS of the reaction mixture recommends that the course of catalysis proceeds through substrate-enzyme adduct formation. Finally, detailed quantum chemical calculations have firmly supported the experimental observations.

Keywords: Bio-inorganic chemistry, cobalt(II), density functional theory, phenoxazinone synthase activity, X-ray structure.

Introduction

Development of structural aspects of cobalt compounds with poly-pyridyl ligands have been a challenging issue in this modern days of science. Cobalt compounds have a valued contributions in the advancement of photophysical and photochemical properties which are extremely demanding in bringing an innovations to different functional materials[1–3]. Cobalt is a bio-essential element that has multi-dimensional effect in this living system. Cobalt is found in cobalamin and in few other metalloproteins[4]. Cobalamin is necessity for building of myelin. Myelin is an insulating layer that available around nerves and support the production of red blood cell which is highly indispensable for the metabolism of fats and carbohydrates, and in the synthesis of proteins[4]. Cobalt ions in association with different poly-pyridyl systems have developed several appealing structural and chemical properties in biological system, therapeutic agents and drug design[5,6]. The oxidative coupling of 2-aminophenol (2-AP) to 2-amino-3*H*-phenoxazine-3-one (APX) through catalytic activation by transition metal complexes has been received

considerable interest since this class of compounds are heading to an important information in bioinorganic chemistry. Exploration of mechanistic aspects for different bio-relevant organic transformations may open a new vista in molecular science[7–9]. 2-Amino-3*H*-phenoxazine-3-one also known as questiomycin A, is related to the naturally occurring antineoplastic agent, actinomycin D. Actinomycin D acts by inhibiting DNA-directed RNA synthesis[10] and is used clinically for the treatment of certain types of cancer[11]. The metallo-enzyme, phenoxazinone synthase catalyzes the oxidative coupling of two molecules of substituted 2-aminophenol to the phenoxazinone chromophore in the final step of the biosynthesis of actinomycin D[12–14]. Although literature survey shows that crystal structure of this cobalt(II) complex was previously reported by Castillo[15] but we follows different kind of reaction methodology to prepare this cobalt(II) complex. To develop a better active catalytic system we use this cobalt(II)-dipyridylamine complex as an efficient bio-mimicking model towards the mimicking of functional site of phenoxazinone synthase enzyme. The cobalt complex significantly promotes the oxidative coupling of 2-aminophenol (2-AP) to 2-

aminophenoxazin-3-one in acetonitrile medium under aerobic condition with turnover number, $k_{cat} = 1.46 \times 10^4 \, h^{-1}$. Theoretical calculations using density functional theory (DFT) further support strongly with the experimental observations.

Results and discussion

Synthesis and spectroscopic characterization:

The Co[II] complex is prepared by addition of 2,2'-dipyridylamine to $Co(NO_3)_2$ in aqueous-methanolic solvent mixture at room temperature. The compound is air-stable and moisture-insensitive. The cobalt(II) complex is soluble in various common solvents like methanol, ethanol, acetonitrile and water.

The IR spectrum of **1** exhibits the presence of characteristic peak at ~1384 cm⁻¹ which is assignable to the existence of NO_3^- anion in **1**. The peaks at 1621 and 1599 cm⁻¹ confirm the presence of imine chromophore of dipyridylamine ligand. Characteristic peaks for the hydrogen atoms of secondary amine-N are clearly observed at ~3327 cm⁻¹ [16]. In order to reveal the spin state conformation, room temperature magnetic measurement is performed. The effective magnetic moment value is found as 4.9 BM which suggests the existence of high spin cobalt(II) centre in solid state. This is slightly higher compare to spin only value for Co[II] ions in high spin state. Probably, $^4T_{1g}$ orbital of Co[II] ions is degenerate that causes a contribution of orbital angular momentum to that magnetic moment.

UV-Vis spectral measurements for **1** in acetonitrile medium are performed at room temperature to examine the solution stability of the complex. Optical bands with higher absorbance at 242, 277, 328 and 431 nm are found. A low intensity but broad electronic transitions at 431 nm attributes to ligand field bands for Co[II] octahedral field[17]. Mass spectral analysis reveals that Co[II] complex produces molecular ion peak at m/z 434.16 (Calcd. 434.12) in methanol as a stable cationic species $[Co(dpa)_2(CH_3OH)]^{2+}$ in solution. This fact is further consolidated by solution conductivity measurement at room temperature in MeOH medium. Conductivity measurement for a $10^{-3} \, M$ solution indicates a 1:2 type electrolyte (119 Scm^2) for this cobalt complex.

Description of X-ray structure:

X-Ray diffraction analysis reveals that the cobalt(II) complex crystallizes in a monoclinic system with $P2_1/n$ space group and exhibits an octahedral geometry. The ORTEP dia-

Table 1. Crystal data and structure refinement parameters for (**1**)

Parameters	(1)
Empirical formula	$C_{20}H_{18}N_8O_6Co$
Formula weight	531.39
Temperature (K)	293
Crystal system	Monoclinic
Space group	$P2_1/n$
a (Å)	17.151(3)
b (Å)	7.3044(12)
c (Å)	17.770(3)
Volume (Å³)	2150.8(6)
Z	4
ρ (g cm⁻³)	1.622
μ (mm⁻¹)	0.856
F (000)	1076
θ ranges (°)	3–27.5
R_{int}	0.368
R (reflections)	22701
w$R2$ (reflections)	4912
Final R indices	0.1530, 0.2281
Largest peak and hole (eA °⁻³)	0.49, –0.42

gram of the cobalt(II) compound is shown in Fig. 1. The crystal structure of the cobalt complex consists of a mononuclear cationic $[Co(2,2'-dpa)_2(NO_3)]^+$ core with nitrate as counter anion. Two units of 2,2'-dpa ligand coordinates Co[II] centre in chelating coordination motifs. Interestingly, nitrate ion plays a pivotal role in the construction of long range crystalline
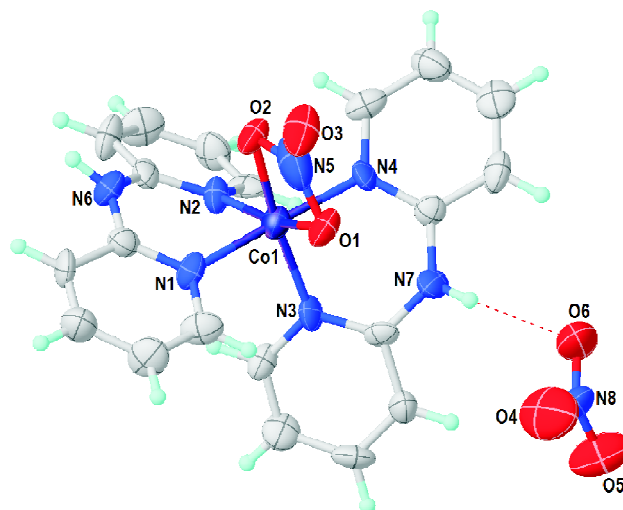

Fig. 1. ORTEP diagram of **1** (30% ellipsoid probability) with atom numbering scheme.

architecture for **1**. Between the two nitrate ions, one behaves as a co-ligand with chelating mode to satisfy the coordination number of Co^{II} centre in the primary zone of coordination while the other nitrate ion acts as a counter anion that helps to neutralize [Co(2,2′-dpa)$_2$(NO$_3$)]$^+$ core. This crystal structure of the cobalt(II) complex was previously published by Castillo[15].

Density functional theory (DFT) of the cobalt(II) complex is also studied to bring additional support for the experimental observations. Gas phase geometric optimization of the cobalt(II) molecular structure (Fig. 2) resembles with the X-ray structure in a high note. The bond distances and angles
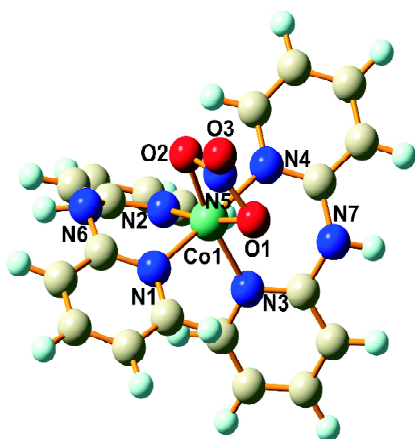

Fig. 2. Optimized structure of Co^{II}-dpa complex in vacuum.

for the optimized molecular structure in gas phase structure (Table 2) also resembles well with the bond connectivity in the crystal structure. The computational outcomes on the molecular structure of Co^{II} complex further unveils that the hexacoordination environment of the cobalt(II) ion in **1** is satisfied by two dpa ligands and one nitrate ion. Each of the dpa units and nitrate ions exhibit the chelation mode of coordination towards Co^{II} ion.

Involvement of H-bonded interactions in the construction of long range 3D crystalline structure is also studied. It is observed that N-H of 2,2′-dpa ligand acts as an acceptor and nitrate ions behave as donor system. Inspite of the existence of two nitrate ions, counter anionic nitrate ion plays a vital role in the construction of 3D crystalline architectures. The counter anionic nitrate contributes each of the oxygen atoms towards H atoms of 2,2′-dpa ligand to make a stronger intermolecular association (Fig. 2). The values of H⋯O interactions range from 2.0 Å to 2.65 Å [C(2)-H(2)⋯O4, 2.38 Å; C(3)-H(3)⋯O5, 2.61 Å; N(7)-H(7)⋯O6; , 2.07 Å Fig. 3] lead to a 3D supramolecular architecture in solid state (Fig. 3).

Phenoxazinone synthase activity:

The aminophenol oxidation activity of the cobalt(II) complex is investigated using 2-aminophenol (2-AP) as a standard substrate in air saturated acetonitrile medium. To perform the investigation, a 1×10^{-3} *M* solution of **1** is treated

Table 2. Selected bond distances (Å) and angles (°) for **1**
(Data within the parenthesis denotes the corresponding theoretical values in vacuum)

| Bond distances (Å)			
Co1-N1	1.947 (1.982)	Co1-N2	1.942 (2.001)
Co1-N4	1.923 (1.940)	Co1-N3	1.910 (1.908)
Co1-O1	1.902 (1.882)	Co1-O2	1.905 (1.880)
Bond angles (°)			
N1-Co1-N2	90.69 (89.88)	N3-Co1-O2	169.02 (172.53)
N1-Co1-N3	92.25 (92.53)	N4-Co1-O1	86.97 (88.89)
N1-Co1-N4	174.65 (172.48)	N4-Co1-O2	86.63 (92.10)
N1-Co1-O1	88.03 (84.89)	N3-Co1-N2	90.22 (90.16)
N1-Co1-O2	88.24 (82.14)	O1-Co1-O2	70.31 (74.27)
N2-Co1-N4	94.56 (95.46)		
N2-Co1-O1	166.22 (168.63)		
N2-Co1-O2	95.94 (95.04)		
N3-Co1-N4	88.30 (92.72)		
N3-Co1-O1	98.75 (99.13)		
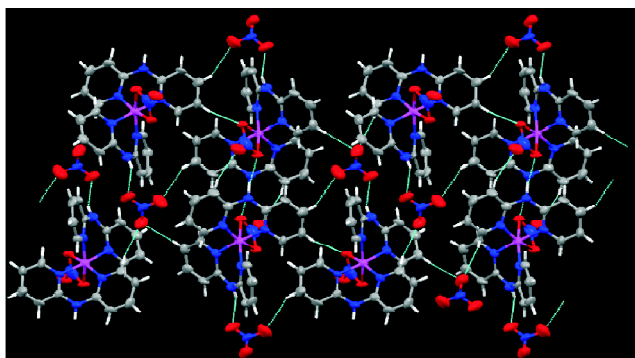
Fig. 3. Nitrate ion mediated 3D crystalline architechture through intermolecular H-bonding interactions.

with 1×10^{-2} *M* of the substrate. The course of the catalytic oxidation reaction is approached through monitoring the optical spectra of the substrate in presence of catalyst at a time interval of 15 min for 3 h.

In order to examine the nature of reactivity for the Co[II]-dpa complex, theoretical calculations have been performed on energy of frontiers orbitals. The electronic transitions involving the frontier orbitals, HOMO→LUMO/HOMO+1/2→LUMO-1/2 (Fig. 4) afford a better view to make an account about the electronic activity. The energy gap between HOMO and LUMO in the cobalt(II)-dpa complex is 2.44 eV which is treated as a lower energy and supports in favour of higher reactivity for the complex.
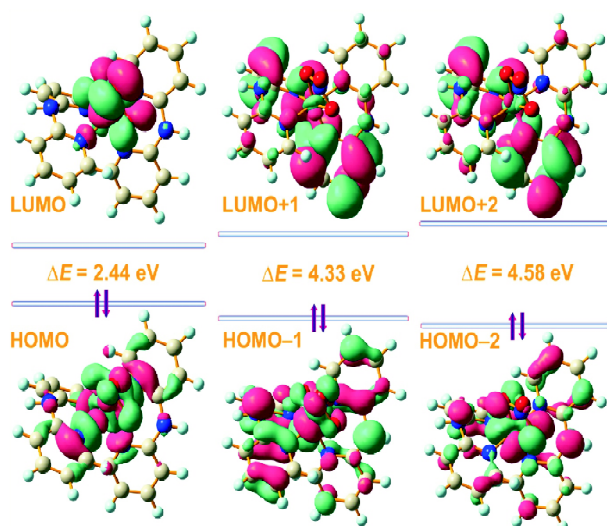

Fig. 4. Graphical plots of the frontier molecular orbitals of Co-dpa complex in IEFPCM/MeCN solvent model with corresponding transition energy values.

The cobalt(II)-dpa complex displays characteristic spectral bands at 242, 277, 328 and 431 nm in the optical spectrum in acetonitrile medium. 2-AP shows a high intensity single band at 267 nm in the UV-Vis spectrum. A gradual decrease in absorbance of the optical band at 267 nm[18–21] is observed with the progress of time and certainly indicates the disappearance of 2-AP from the solution. During the course of catalysis, an initial new broad band with increasing intensity is concomitantly formed in the region 385–410 nm centred at 398 nm[21,22] (Fig. 5). An additional new optical band is also found in the spectral region 690–710 nm[20–22] which presents an indication about the formation of cobalt ion-2-AP adduct in the solution. The phenomenon with the
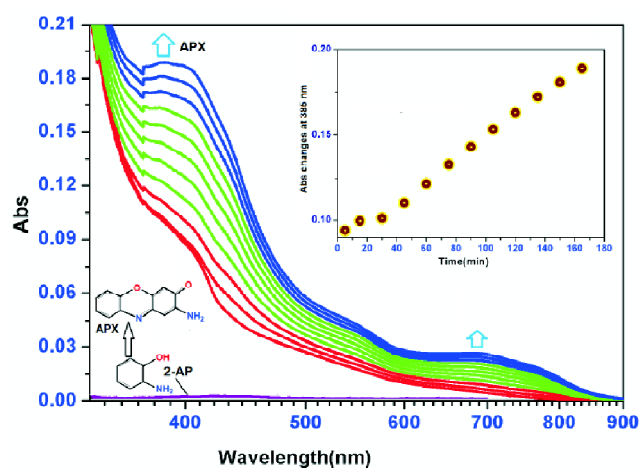

Fig. 5. Increase of optical band at 398 nm upon addition of 10 equivalents of **1** (10^{-3} *M*) to 100 equivalent of 2-AP in MeCN [The spectra were recorded after every 15 min]. Inset: Time vs absorbance plot.

appearance of an optical band at ~398 nm accounts for the catalytic conversion of 2-AP to phenoxazinone species in acetonitrile solution. Blank experiment in acetonitrile in absence of cobalt(II)-dpa complex under similar experimental condition didn't produced any phenoxazinone species and signify the presence of cobalt(II)-dpa complex in this catalytic oxidation reaction. The phenoxazinone compound is purified and extracted by column chromatography. The isolated product is found in high yield (84.1% for **1**). The product was identified by ^{1}H NMR spectroscopy. ^{1}H NMR (CDCl$_3$, 500 MHz) δ_H: 7.66 (m, 1H), 7.42 (m, 3H), 6.49 (s, 1H), 6.36 (s, 1H).

Kinetic studies for the catalytic oxidation of 2-AP are studied to comprehend the extent of catalytic efficiency. The kinetics of catalytic oxidation of 2-AP are determined following the method of initial rates. The catalytic oxidation reactions are monitored with the growth of phenoxazinone species at 398 nm as a function of time[22,23] (Fig. 6). The values of kinetics parameters are determined by analyzing the plot of the rate constants versus concentration of 2-AP plot based on the Michaelis-Menten approach of enzymatic kinetics (Fig. 6). The values of kinetics parameters are V_{max}, 4.06×10^{-5}, Sd. error 6.86×10^{-6}; K_M, 6.49×10^{-3}, Sd. error 2.24×10^{-4} and k_{cat}, 1.46×10^4 h^{-1}.

To assess the mechanistic routes for this catalytic oxidation by cobalt(II) complex towards 2-AP, *in situ* mass spectral analysis of 2-AP in presence of **1** in acetonitrile medium is perf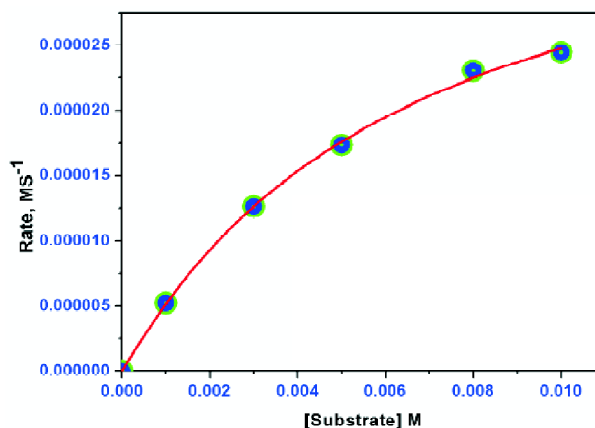ormed. ESI-MS spectral analysis for that reaction mixture (Fig. 7) in acetonitrile medium exhibits mainly the characteristics peaks at *m/z* 216.09 and 510.63 with isotope distri-

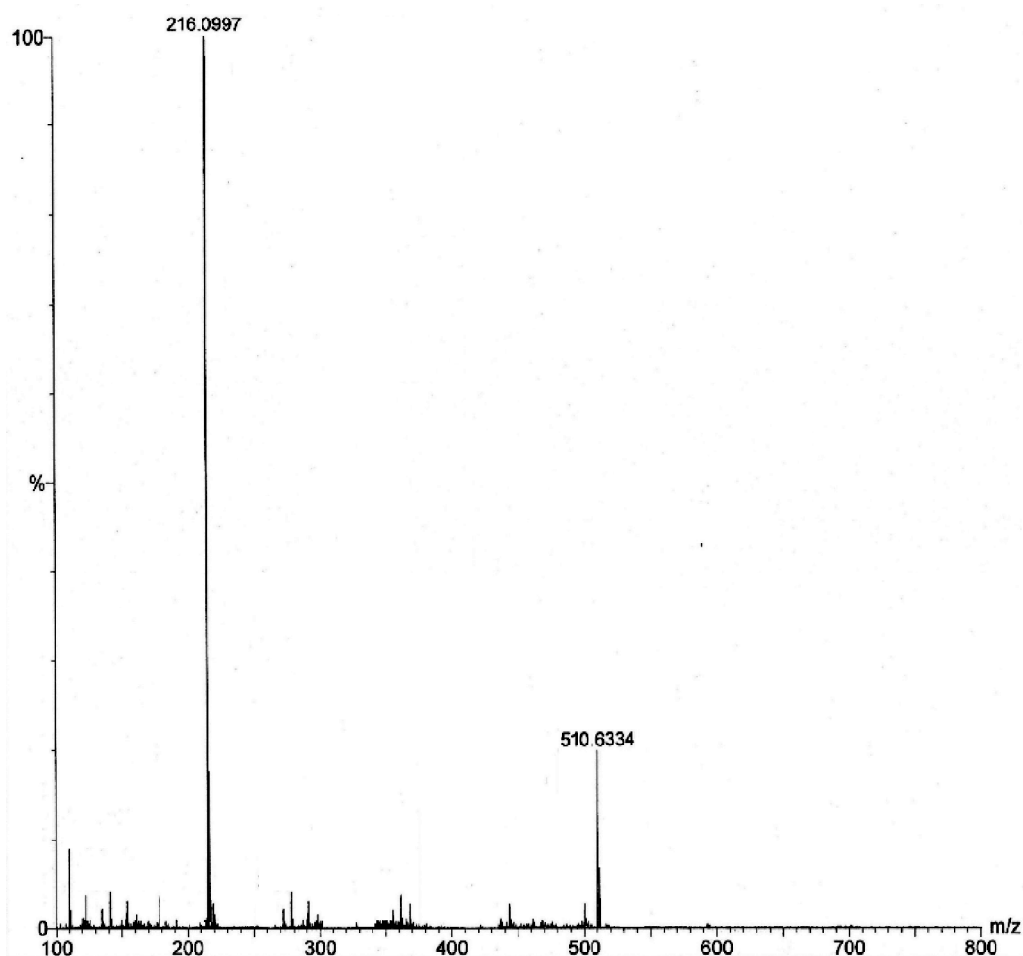**Fig. 6.** Plot of rate versus [substrate] in presence of **1** in MeCN.

Fig. 7. ESI-Mass spectrum of the reaction mixture of **1** with 2-AP in MeCN.

bution patterns which consolidates the presence of [(2-amino-3*H*-phenoxazine-3-ones) + H$^+$] and [[Co(2-amino-phenol)(dpa)$_2$] + H$^+$] species respectively. Further, the characteristic peak at *m/z* 510.63 confirms the existence of substrate-catalyst adduct in solution in the form of coordinated iminobenzosemiquinonato to cobalt ion in the course of catalysis. From the *in situ* mass spectrum, it can be recommended that the course of catalysis is occurred through substrate-catalyst adduct formation (Scheme 1).
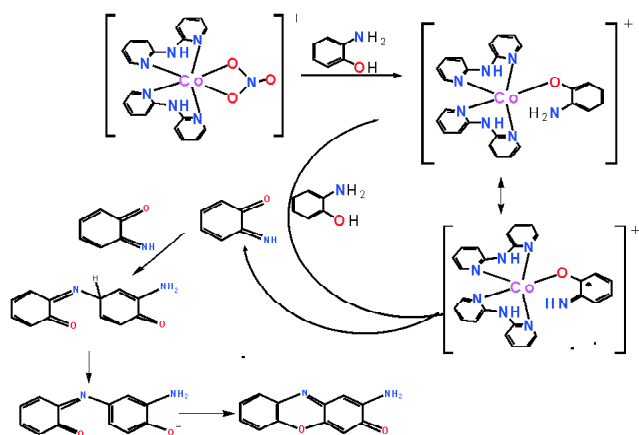
Scheme 1. Proposed mechanistic pathways for aminophenol oxidation by cobalt(II) complex.

Conclusion

A mononuclear cobalt(II) complex with dipyridylamine ligand has been synthesized and isolated in good yield. The cobalt(II) compound contains two nitrate ions with different coordination motifs – first one is for the saturation of the coordination number and the second one is for charge balance. Strong intermolecular H-bonding interactions between counter anionic nitrate and dpa ligand play a pivotal role in the construction of long range 3D crystalline structure. Computation modelling strongly supports the structural aspects of X-ray structure and accounts for its high reactivity in solution. The cobalt(II) complex has been evaluated to mimics phenoxazinone synthase enzyme and significantly promotes the catalytic oxidation of 2-aminophenol (2-AP) to 2-aminophenoxazin-3-one in acetonitrile medium under aerobic condition with turnover number, k_{cat} = 1.46×10^4 h^{-1}. The cobalt(II) based catalytic oxidation follows a saturation kinet-

ics and proceeds through catalyst-substrate intermediate with high catalytic efficacy.

Experimental

Chemicals, solvents and starting materials:

High purity 2,2′-dipyridylamine (Lancaster, UK), cobalt(II) nitrate hexahydrate (E. Merck, India), 2-aminophenol (Aldrich, UK), were purchased and used as received. All the other reagents and solvents were of analytical grade (AR grade) purchased from commercial sources and were used as received.

Synthesis of [Co(2,2′-dpa)$_2$(NO$_3$)]NO$_3$ (1):

A 50-50 v/v MeOH-H$_2$O solution (10 mL) of 2,2′-dipyridylamine (0.1710 g, 1 mmol) was added drop wise to a solution of Co(NO$_3$)$_2$.6H$_2$O (0.2880 g, 1 mmol) in the same solvent (10 mL) and mixed slowly on a magnetic stirrer with slow stirring for 10 min. Then the solution was refluxed for another 30 min. Lastly, the pink coloured solution was filtered and the supernatant liquid was kept in air for slow evaporation. After a few days, the fine microcrystalline compound that separated out was washed with toluene and dried *in vacuo* over silica gel indicator.

Yield: 0.1910 g (66.3% based on metal salt). Anal. (%): Calcd. for C$_{20}$H$_{18}$N$_8$O$_6$Co (1): C, 45.73; H, 3.45; N, 21.33. Found: C, 45.80; H, 3.39; N, 21.40; IR (KBr pellet, cm^{-1}): 3338, 1626, 1598, 1384; UV-Vis (λ, nm, 10^{-4} *M*): 242, 277, 328, 431.

Physical measurements:

Infrared spectrum was recorded with a FTIR-8400S Shimadzu spectrophotometer using KBr pellet in the range 400–3600 cm^{-1}. Ground state absorption was measured with a JASCO V-730 UV-Vis spectrophotometer. Elemental analyses were performed on a Perkin-Elmer 2400 CHN microanalyser. Electrospray ionization (ESI) mass spectrum was recorded using a Q-tof-micro quadruple mass spectrometer. Solution conductivity was recorded using a Systronic conductivity meter. A Gouy balance was used to determine room temperature magnetic susceptibility of the powdered sample. Diamagnetic corrections were made from the Pascal's constants.

Single crystal X-ray diffraction study:

Single crystal X-ray diffraction data of the cobalt complex were collected using a Rigaku XtaLABmini diffractometer

equipped with mercury CCD detector. The data were collected with graphite monochromated Mo-Kα radiation (λ = 0.71073 Å) at 293(2) K using ω scans. The data were reduced using Crystal Clear suite 2.0[24] and the space group determination was done using Olex2[25]. The structure was resolved by direct method and refined by full-matrix least-squares procedures using the SHELXL-2014/7[26] software package using Olex2 suite. Tables 1 and 2 lists all the crystallographic and bond angles, bond distance parameters related to the crystal structure reported herein.

Catalytic oxidation of 2-aminophenol:

In order to examine phenoxazinone synthase activity, 1×10^{-4} *M* solution of **1** in acetonitrile medium is treated with 10 equivalent of 2-aminophenol (2-AP) under aerobic conditions at room temperature. Absorbance vs wavelength (wavelength scans) of these solutions are recorded at a regular time interval of 15 min for aminophenol oxidation in the wavelength range 300–800 nm[18–21].

Kinetic experiments were performed spectrophotometrically with complex **1** and 2-AP in acetonitrile at 25°C for aminophenol oxidation activity 0.04 mL of the complex solution, with a constant concentration of 1×10^{-4} *M*, was added to 2 mL of 2-AP of a particular concentration (varying its concentration from 1×10^{-3} *M* to 1×10^{-2} *M*) to achieve the ultimate concentration of the complex as 1×10^{-4} *M*. The conversion of 2-aminophenol to 2-aminophenoxazine-3-one was monitored with time at a wavelength 398 nm (time scan) in MeCN[22,23].

Computational details:

To provide strong support to the experimental findings, extensive quantum mechanical calculations have been performed using Gaussian 09 program suite[27]. GaussView 5.0.8[27] has been widely used for visualisation and image extraction purpose. The ground-state and excited state calculations have been operated with density functional theory (DFT) and time dependent density functional theory (TD-DFT) respectively in conjugation with B3LYP theoretical model and 6-311G basis set[28]. This B3LYP is an well established theoretical model for quantum chemical calculations[29–33] in vacuum and as well as in various solvents. Initially, the Co^{II} complex have been optimized in vacuum. Thereafter, to be consistent with the experimental observations, the Co^{II} complex has been optimized in methanol (ε = 32.613) following Integral Equation Formalism Polarisable continuum Model

(IEFPCM)[34–37]. To confirm the optimized structure to be true minima, the stability of the optimized structure has been verified through IR frequency and stability calculations. The bond length and bond angle parameters of the optimized structure in vacuum resemble very well with the single crystal XRD structure of the Co^{II} complex.

Acknowledgement

References

1. M. E. Reichmann, S. A. Rice, C. A. Thomas and P. Doty, *J. Am. Chem. Soc.*, 1954, **76**, 3047.

2. D. Lahiri, R. Majumdar, A. K. Patra and A. R. Chakravarty, *J. Chem. Sci.*, 2010, **122**, 321.

3. D. Dey, A. De, S. Pal, P. Mitra, A. Ranjani, L. Gayathri, S. Chandraleka, D. Dhanasekaran, M. A. Akbarsha, N. Kole and B. Biswas, *Indian J. Chem.*, 2015, **54A**, 170.

4. B. N. Trawick, A. T. Daniherl and J. K. Bashkin, *Chem. Rev.*, 1998, **98**, 939.

5. P. G. Sammes and G. Yahioglu, *Chem. Soc. Rev.*, 1994, **23**, 327.

6. D. Dey, A. Basu Roy, C.-Y. Shen, H.-L. Tsai, A. Ranjani, L. Gayathri, S. Chandraleka, D. Dhanasekaran, M. A. Akbarsha, N. Kole and B. Biswas, *J. Chem. Sci.*, 2015, **127**, 649.

7. J. McLain, J. Lee and J. T. Groves, in: B. Meunier (Ed.), "Biomimetic Oxidations Catalyzed by Transition Metal Complexes", Imperial College Press, London, 2000.

8. F. Benedini, G. Galliani, M. Nali, B. Rindone and S. Tollari, *J. Chem. Soc., Perkin Trans.*, 1963, **2**, 1985.

9. L. I. Simándi, S. Németh and N. Rumlis, *J. Mol. Catal.*, 1987, **42**, 357.

10. Z. Szeverényl, E. R. Mileava and L. I. Simándi, *J. Mol. Catal.*, 1991, **67**, 251.

11. S. Sakaue, T. Tsubakino, Y. Nishiyama and Y. Ishii, *J. Org. Chem.*, 1993, **58**, 3633.

12. J. Kaizer, R. Csonka and G. Speier, *J. Mol. Catal. A: Chem.*, 2002, **180**, 91.

13. T. Horvath, J. Kaizer and G. Speier, *J. Mol. Catal. A: Chem.*, 2004, **215**, 9.

14. M. R. Maurya, S. Sikarwar, T. Joseph and S. B. Halligudi, *J. Mol. Catal. A: Chem.*, 2005, **236**, 132.

15. O. Castillo A. Luque, Pinta, NDL and Roman Pascual, *Acta Cryst. E*, 2001, **57**, 384.

16. (a) K. Nakamoto, "Infrared and Raman Spectra of Inorganic and Coordination Compounds. Part B: Applications

in Coordination, Organometallic, and Bioinorganic Chemistry", 6th ed., John Wiley & Sons Inc, New Jersey, 2009; (b) D. Dey, G. Kaur, M. Patra, A. R. Choudhury, N. Kole and B. Biswas, *Inorg. Chim. Acta*, 2014, **421**, 335.

17. J. G. Sole, L. E Bausa and D. Jaque, "An Introduction to Optical Spectroscopy of Inorganic solids", John Wiley & Sons Ltd., 2005.

18. S. K. Dey and A. Mukherjee, *Coord. Chem. Rev.,* 2015, **310**, 80.

19. T. M. Simándi, L. I. Simándi, M. Győr, A. Rockenbauer and A. Gömöry, *J. Chem. Soc., Dalton Trans*., 2004, **1056**, 15.

20. I. C. Szigyártó, T. M. Simándi, L. I. Simándi, L. Korecz and N. Nagy, *J. Mol. Catal. A: Chem.,* 2006, **251**, 270.

21. P. Mialane, L. Tehertanov, F. Banse, J. Sainton and J. Girerd, *Inorg. Chem*., 2000, **39**, 2440.

22. D. Dey, G. Kaur, A. Ranjani, L. Gyathri, P. Chakraborty, J. Adhikary, J. Pasan, D. Dhanasekaran, A. R. Choudhury, M. A. Akbarsha, N. Kole and B. Biswas, *Eur. J. Inorg. Chem*., 2014, 3350.

23. A. Panja and T. K. Mandal, *Indian J. Chem*., 2016, **55A**, 137.

24. CrystalClear 2.0, Rigaku Corporation, Tokyo, Japan.

25. G. M. Sheldrick, *Acta. Cryst*., 2008, **A64**, 112.

26. L. J. Farrugia, ORTEP-32 for Windows, University of Glasgow, Scotland, 1998.

27. M. J. Frisch, G. W. Trucks, H. B. Schlegel, G. E. Scuseria, M. A. Robb, J. R. Cheeseman, G. Scalmani, V. Barone, B. Mennucci, G. A. Petersson, H. Nakatsuji, M. Caricato, X. Li, H. P. Hratchian, A. F. Izmaylov, J. Bloino, G. Zheng, J. L. Sonnenberg, M. Hada, M. Ehara, K. Toyota, R. Fukuda, J. Hasegawa, M. Ishida, T. Nakajima, Y. Honda, O. Kitao, H. Nakai, T. Vreven, J. A. Montgomery, J. E. Peralta (Jr.), F. Ogliaro, M. Bearpark, J. J. Heyd, E. Brothers, K. N. Kudin, V. N. Staroverov, R. Kobayashi, J. Normand, K. Raghavachari, A. Rendell, J. C. Burant, S. S. Iyengar, J. Tomasi, M. Cossi, N. Rega, J. M. Millam, M. Klene, J. E. Knox, J. B. Cross, V. Bakken, C. Adamo, J. Jaramillo, R. Gomperts, R. E. Stratmann, O. Yazyev, A. J. Austin, R. Cammi, C. Pomelli, J. W. Ochterski, R. L. Martin, K. Morokuma, V. G. Zakrzewski, G. A. Voth, P. Salvador, J. J. Dannenberg, S. Dapprich, A. D. Daniels, O. Farkas, J. B. Foresman, J. V. Ortiz, J. Cioslowski and D. J. Fox, Gaussian 09 (Revision A.02), Gaussian, Inc., Wallingford, CT, 2009.

28. Y. Zhao and D. G. Truhlar, *J. Chem. Phys*., 2006, **125**, 194101.

29. M. Karar, S. Paul, B. Biswas, T. Majumdar and A. Mallick, *Dalton Trans*., 2018, **47**, 7059.

30. M. Karar, S. Paul, A. Mallick and T. Majumdar, *ChemistrySelect*, 2017, **2**, 2815.

31. S. Paul, M. Karar, S. Mitra, S. A. S. Shah, T. Majumdar and A. Mallick, *ChemistrySelect*, 2016, **1**, 5547.

32. S. Paul, M. Karar, B. Das, A. Mallick and T. Majumdar, *Chem. Phys. Lett*., 2017, **689**, 199.

33. S. Paul, A. Mallick and T. Majumdar, *Chem. Phys. Lett*., 2015, **634**, 29.

34. B. Mennucci, E. Cances and J. Tomasi, *J. Phys. Chem. B*, 1997, **101**, 10506.

35. E. Cances, B. Mennucci and J. Tomasi, *J. Chem. Phys*., 1997, **107**, 3032.

36. R. Cammi and J. Tomasi, *J. Comput. Chem*., 1995, **16**, 1449.

37. S. Miertus, E. Scrocco and J. Tomasi, *J. Chem. Phys*., 1981, **55**, 117.